

Magnetic Properties of Ball-Milled Nanocrystalline Alloys $\text{Fe}_{78}\text{B}_{13}\text{Si}_9$

Marek Pekala^{1,*}, Jan Grabski², and Martyna Jachimowicz³

¹ Chemistry Department, Warsaw University, PL-02089 Warsaw, Poland

² Physics Department, Warsaw University of Technology, PL-00662 Warsaw, Poland

³ Department of Materials Science and Engineering, Warsaw University of Technology, PL-02524 Warsaw, Poland

Summary. Magnetic properties of nanocrystalline $\text{Fe}_{78}\text{B}_{13}\text{Si}_9$ alloys are studied for three series prepared by ball milling starting from amorphous ribbons, crystallized ribbons, and elemental powders. Temperature variation of static magnetization results in strong ferromagnetic interaction which is weakly dependent on the initial material. Magnetic hysteresis loops show that saturation magnetization, magnetic remanence, and coercive field increase with frequency for both series of ribbon samples, whereas they decrease for alloys prepared from elemental powders. Power losses raise faster for the alloys prepared from elemental powders than for the two other alloys.

Keywords. Nanostructures; Alloys; Magnetic properties; Solid state synthesis.

Introduction

Nanotechnology offers new routes to synthesize new materials as well as to modify materials of classical chemical composition. The unique properties of such materials are due to a specific internal structure composed of grains of nanometer size. A remarkable amount of atoms is located at grain surfaces; their local structural and chemical coordination may be different from those in the grain cores. Depending on the way of synthesis, up to 50% of the atoms may occupy such surface or grain boundary sites. This in turn determines physical properties of the nanomaterials [1].

The above considerations raise the important question how properties are affected by the initial state of the materials from which the nanoproducts are prepared, especially when the ball milling technique is used. In order to compare the properties of final nanomaterials, $\text{Fe}_{78}\text{B}_{13}\text{Si}_9$ alloys were selected and processed in various ways. Amorphous alloys of the same composition have been studied several years ago as potential transformer cores [2–4]. As the applicability range is determined by magnetization, coercivity, and power loss properties, a response of these alloys to magnetic fields is studied at various frequencies. The observed hysteresis arises from the fact that the non-equilibrium magnetic system in alloys is moved around in phase space by an external magnetic field [5].

* Corresponding author. E-mail: pekala@chem.uw.edu.pl

Results and Discussion

The experimental results show that high-energy ball milling produces a nanocrystalline structure for all starting materials studied. The average final crystallite sizes are about 8 to 16 nm. Structural evolution of alloys occurring during the milling process affects the magnetic properties of the alloys.

All alloys studied exhibit a strong ferromagnetic ordering, independent of the starting material. The room temperature values of static magnetization of the *K* and *P* alloys are in the range of 180 to 189 $\text{A} \cdot \text{m}^2/\text{kg}$ depending on milling time. Typical magnetization curves of *P* alloys are shown in Fig. 1. The *A* alloys exhibit a somewhat smaller room temperature magnetization of 180 $\text{A} \cdot \text{m}^2/\text{kg}$. The *Curie* temperature of the nanocrystalline phases determined from temperature variation of magnetization amounts to 1050 K and confirms strong magnetic interactions. Temperature variation of magnetization allows to detect the presence of various magnetic phases as well as their respective *Curie* temperatures. The magnetic hysteresis loops registered at room temperature show a smooth evolution of magnetization, coercivity, and power losses with milling time.

Saturation magnetization of the *K* alloys is spread up to 0.18 T depending on frequency and increases with milling time (Fig. 2). For these alloys containing a mixture of $\alpha\text{-Fe}(\text{Si})$ and Fe_2B phases, the parallel increase of magnetic remanence and coercive field with milling time can be seen from Figs. 3 and 4. For the longest milling time of 450 h, when the alloys attain the nanocrystalline structure, saturation magnetization and coercive field increase approximately twice upon varying the frequency from 50 to 50000 Hz (Figs. 2 and 4). Figure 5 shows that also the power losses increase abruptly with milling time. The coercive fields and power

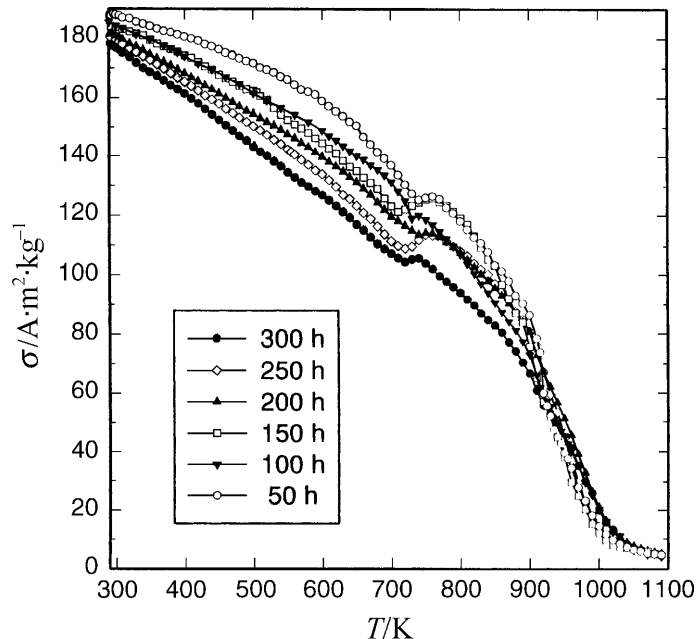


Fig. 1. Temperature variation of mass magnetization for $\text{Fe}_{78}\text{B}_{13}\text{Si}_9$ alloys *P* prepared from a mixture of elemental powders at various milling times

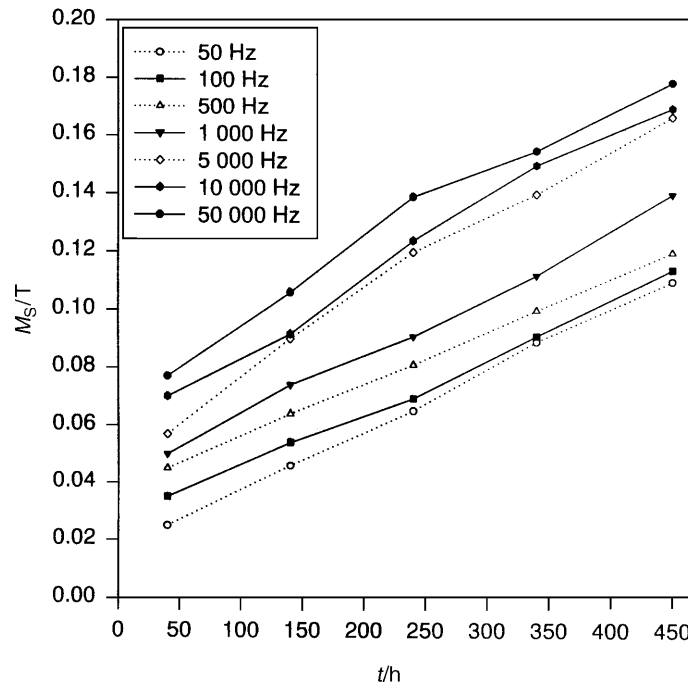


Fig. 2. Variation of saturation magnetization with milling time at various frequencies for alloys K prepared from crystallized ribbons

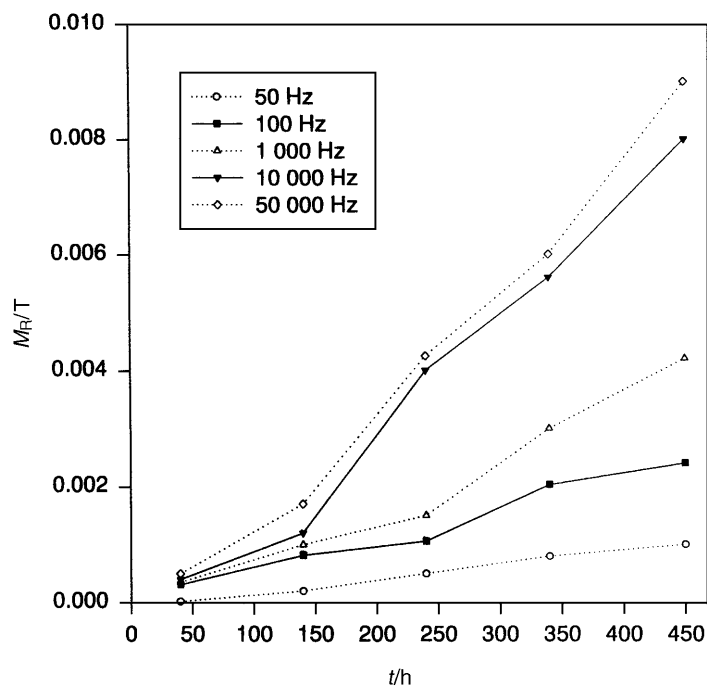


Fig. 3. Variation of magnetic remanence with milling time at various frequencies for alloys K prepared from crystallized ribbons

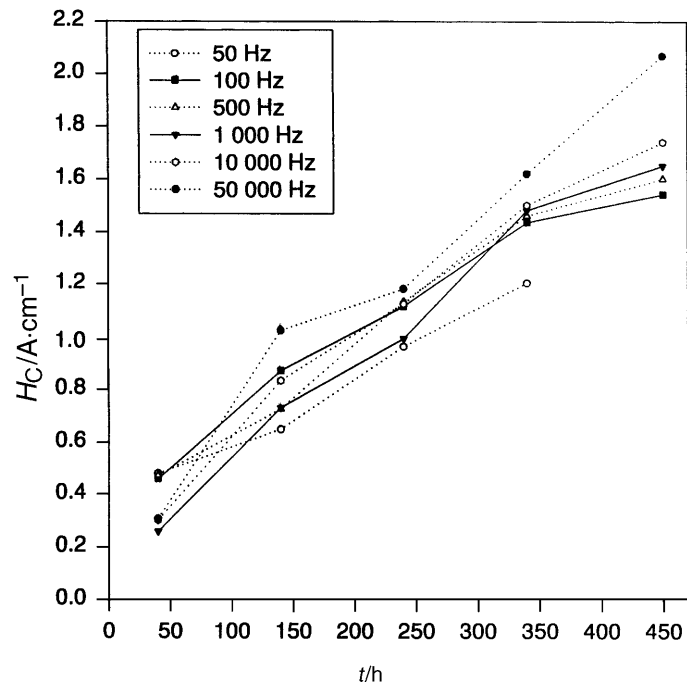


Fig. 4. Variation of coercive field with milling time at various frequencies for alloys *K* prepared from crystallized ribbons

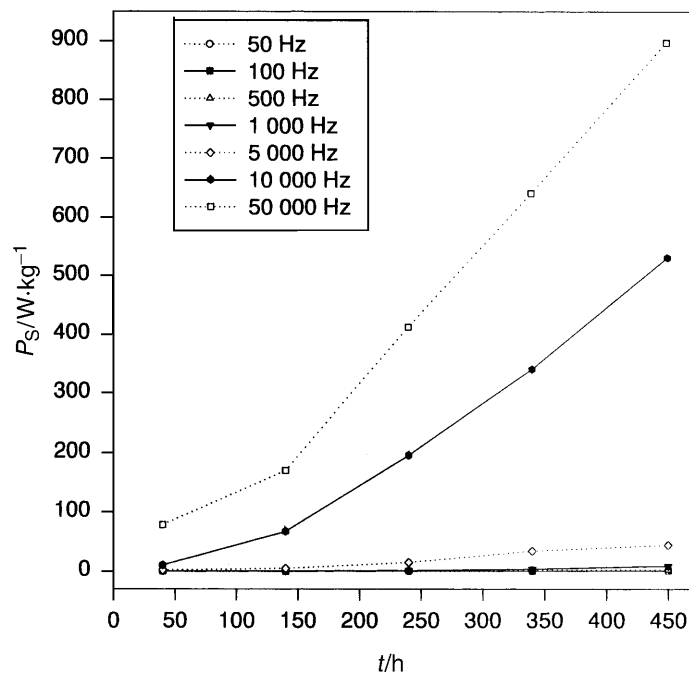


Fig. 5. Variation of power losses with milling time at various frequencies for alloys *K* prepared from crystallized ribbons

losses increase also for P alloys; in these alloys, the Si atoms are dissolved, and the B atoms migrate into the iron lattice.

The above described behaviour is in contrast to that of A alloys, in which saturation magnetization, magnetic remanence, and coercive field diminish with milling time. On the other hand, power losses increase with milling time. Such a behaviour is related to a decay of the amorphous phase. The nanocrystalline structure made up from $\alpha\text{-Fe}(\text{Si})$ and Fe_2B phases develops during the milling process. This transformation from the amorphous to the nanocrystalline phase has been confirmed by magnetization curves and *Moessbauer* spectroscopy [7].

The oscillating magnetic field strongly influences coercivity and magnetic losses in the alloys studied. Saturation magnetization and magnetic remanence increase monotonically with frequency for A and K alloys (Figs. 6 and 7), whereas these parameters diminish for the P alloys. Coercivity increases with frequency in A and K alloys as shown in Fig. 8. The same tendency has been reported for amorphous Fe-based alloys [8]. Figure 8 also shows that the coercive field of the P alloys decreases with increasing frequency.

Magnetic losses P_S raise with frequency as shown in Fig. 9 for the three alloy series. Absolute values of P_S are of the same order of magnitude in the A and K alloys when compared at the same frequency and agree with values reported for $\text{Fe}_{78}\text{B}_{13}\text{Si}_9$ alloys [9–13]. At lower frequencies, values of P_S are about one order of magnitude smaller for the P alloys.

In soft magnetic materials, magnetic losses are composed of two contributions. The first one is related to hysteresis losses occurring due to reordering of magnetic domain structures in an oscillating magnetic field and is approximately

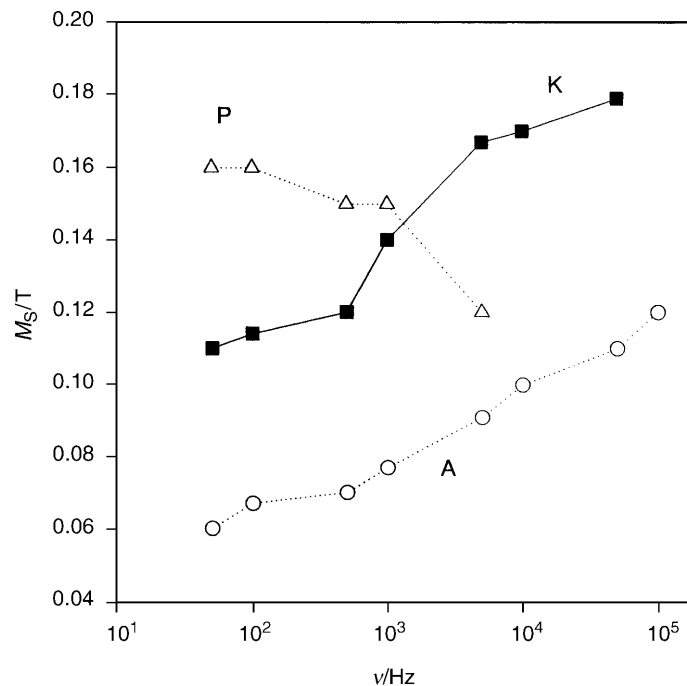


Fig. 6. Frequency dependence of magnetization for A , K , and P alloys

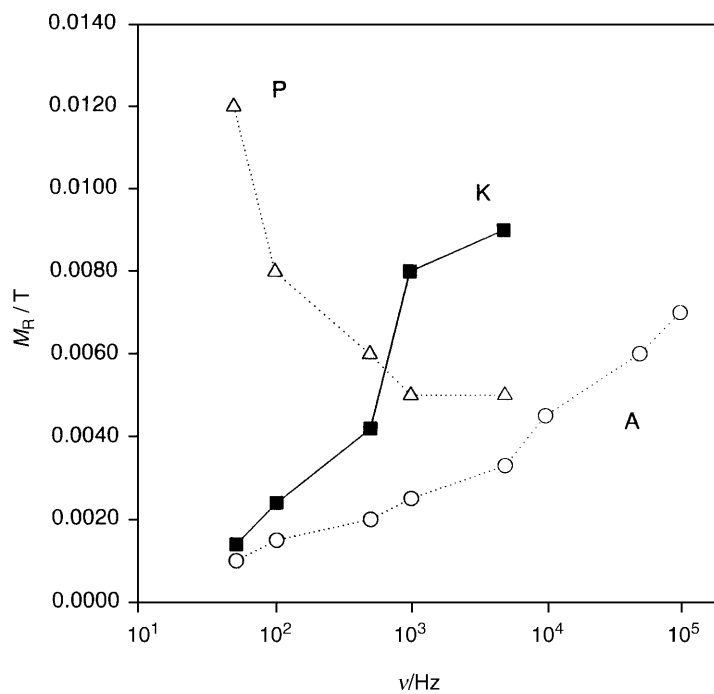


Fig. 7. Frequency dependence of magnetic remanence for A, K, and P alloys

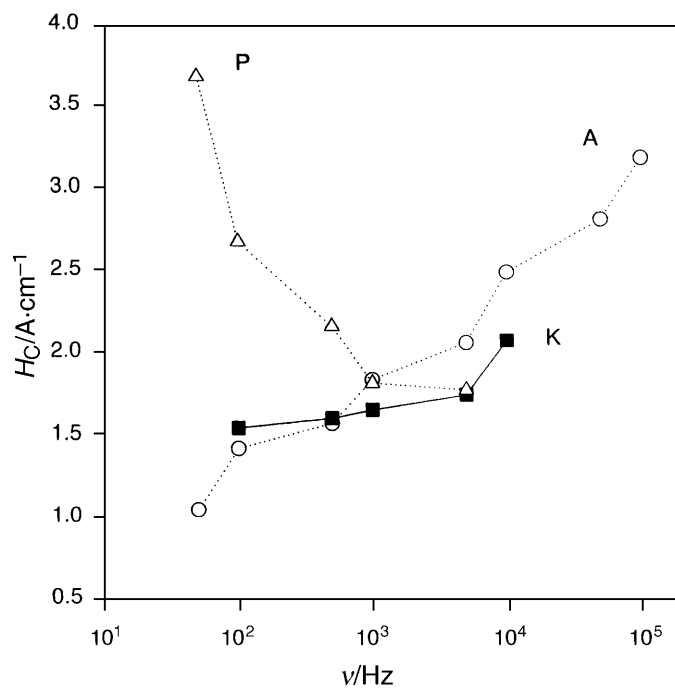


Fig. 8. Frequency dependence of coercive field for A, K, and P alloys

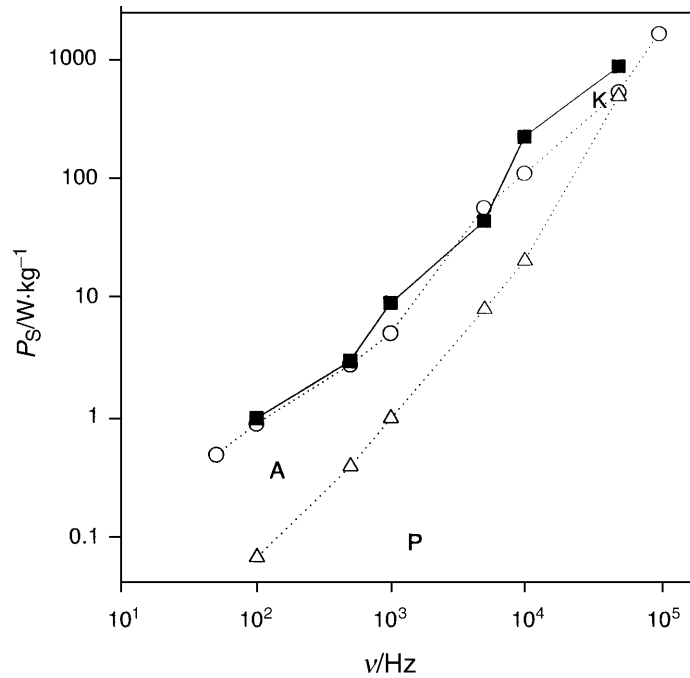


Fig. 9. Frequency dependence of power losses for A, K, and P alloys

proportional to the frequency ν [14, 15]. For $\text{Fe}_{74.5}\text{Cu}_{0.75}\text{Nb}_{2.25}\text{Si}_{13.5}\text{B}_9$, losses have been approximated by ν^z , z ranging between 1.3 and 1.8 [16]. The second contribution, related to eddy current losses, is proportional to ν^2 [9, 14] and dominates at higher frequencies. Plots of power losses vs. frequency allow to calculate the exponents governing these dependences. The values of z are very close to 1 for the A and K alloys, whereas for P alloys this exponent amounts to about 1.3.

Frequency variation of magnetic loop parameters is related to the rate dependent hysteresis of the magnetic system, which is driven both by the external magnetic field and thermal excitations. A response (accommodation) of the magnetic system to the actual magnetic field depends on the height of energy barriers and the rate of thermal relaxation occurring at given frequency.

The ball milling route was found to be an effective way to produce nanocrystalline alloys with properties required for practical applications; the distribution of magnetic parameters depends only weakly on the form of starting materials used for the synthesis of the alloys.

Experimental

The ball milling procedures were applied to three materials of the composition $\text{Fe}_{78}\text{B}_{13}\text{Si}_9$: amorphous ribbons, crystallized ribbons, and a mixture of elemental crystalline powders. Amorphous ribbons with a thickness about 0.02 mm produced by the melt spinning technique were cut into pieces of about 5×5 mm. Part of the ribbon was fully crystallized by annealing at 900 K for 1 h. Both the amorphous and crystallized ribbons were initially broken and used as starting materials for the ball milling procedure, which produced the 'A' and 'K' alloys, respectively. As a third starting

material, a mixture of crystalline powders of desired atomic composition, resulted in the 'P' alloys. The ball milling was performed in a vibratory mill under Ar. Stainless steel vials and balls were used. The weight ratio of balls to milled material was 5:1. During milling, small quantities of powder were removed from the vial in a glove-box filled with Ar. More details of the preparation are described in Refs. [6, 7].

X-Ray diffraction (XRD) and differential scanning calorimetry (DSC) were used for alloy characterization. Contamination mainly by oxygen and iron originating from the milling process did not exceed 2 at.%. The lattice parameters were determined from the diffraction patterns by least square fitting with employing an angle correction function. Mean crystallite size D and average microstrain were calculated using the *Cauchy-Gauss* method with errors not exceeding 10 and 15%, respectively. Static magnetization measurements were made with a *Faraday* balance with an accuracy of below 1%. Magnetic hysteresis loops were recorded over a broad frequency range (50 to 400 000 Hz) at magnetic field amplitudes of 500 and 5000 A/m.

Acknowledgments

This work was supported in part by grant No. 120-501/SPUB-77.

References

- [1] Inoue A (2000) *Acta Mater* **48**: 279
- [2] Kunitomo N (1994) *Mater Sci Eng* **A181–182**: 1296
- [3] Dmowski R, Puzniak R (1984) *Acta Magn (PL) Suppl* 244
- [4] Allia P, Baricco M, Vinai F (1990) *J Magn Magn Mat* **83**: 347
- [5] Bertotti G, Basso C, Beatrice C, LoBue M, Magni A, Tiberto P (2001) *J Magn Magn Mat* **226–230**: 1206
- [6] Pekala M, Jachimowicz M, Fadeeva VI, Matyja H, Grabias A (2001) *J Non-Crystalline Solids* **287**: 380
- [7] Pekala M, Jachimowicz M, Fadeeva VI, Matyja H (2001) *J Non-Crystalline Solids* **287**: 360
- [8] Zhukov A, Vazquez M, Velazquez J, Garcia C, Valenzuela R, Ponomarev B (1997) *Mater Sci Eng* **A226–228**: 753
- [9] Warlimont H (2001) *Mater Sci Eng* **A304–306**: 61
- [10] Yoshizawa Y, Oguma S, Yamauchi K (1988) *J Appl Phys* **64**: 6044
- [11] Makino A, Suzuki K, Inoue A, Hirotsu Y, Masumoto T (1994) *J Magn Magn Mat* **133**: 329
- [12] Makino A, Bitoh T, Kojima A, Inoue A, Masumoto T (2001) *Mater Sci Eng* **A304–306**: 1083
- [13] del Real RP, Prados C, Pulido E, Hernando A (1993) *J Appl Phys* **73**: 6618
- [14] Luborsky FE (1980) In: Wohlfarth EP (ed) *Ferromagnetic Materials*, vol 1. North-Holland, Amsterdam, p 451
- [15] McHenry ME, Willard MA, Laughlin DE (1999) *Progress in Mater Sci* **44**: 291
- [16] Schaefer M, Dietzmann G (1994) *J Magn Magn Mater* **133**: 303

Received October 5, 2001. Accepted (revised) November 12, 2001